PACS numbers: 42.25.Dd; 87.50.Hj, 87.64.Cc
DOI: 10.1070/QE2001v031n12ABEH002108

Monte Carlo simulation of reflection spectra of random multilayer media strongly scattering and absorbing light

I V Meglinskii

***Abstract*. The reflection spectra of a multilayer random medium – the human skin – strongly scattering and absorbing light are numerically simulated. The propagation of light in the medium and the absorption spectra are simulated by the stochastic Monte Carlo method, which combines schemes for calculations of real photon trajectories and the statistical weight method. The model takes into account the inhomogeneous spatial distribution of blood vessels, water, and melanin, the degree of blood oxygenation, and the hematocrit index. The attenuation of the incident radiation caused by reflection and refraction at Fresnel boundaries of layers inside the medium is also considered. The simulated reflection spectra are compared with the experimental reflection spectra of the human skin. It is shown that a set of parameters that was used to describe the optical properties of skin layers and their possible variations, despite being far from complete, is nevertheless sufficient for the simulation of the reflection spectra of the human skin and their quantitative analysis.**

Keywords: *reflection spectrum of skin, Monte Carlo method, tissue optics.*

1. Introduction

The development and the use of contactless methods of optical diagnostics for studies in biology and medicine are one of the important trends in modern optics [1, 2]. Of special interest is the application of contactless optical methods for diagnostics and control of the parameters of the bloodstream and skin pigmentation. Although the melanin pigment and capillary loops are not deeply located beneath the skin surface (20 – 100 μm and 100 – 200 μm, respectively), the solution of this problem is far from trivial. This is explained by strong scattering and absorption of light by the upper layers of the skin caused by the inhomogeneous distribution of blood vessels [3, 4], melanin [5], and other chromophores [6] over the depth beneath the skin surface. As a result, the quantitative measurement of the content of these components in the skin is very complicated because it is very difficult to decompose the reflection spectra into components corresponding to the absorption spectra of individual chromophores involved in the measurements.

At present, the reflection spectroscopy is the most popular method for optical diagnostics of the skin [2, 7 – 9]. This method is based on a comparative analysis of the reflection spectra obtained for healthy and diseased* skin regions. The use of simplified skin models [7 – 10] and mathematical methods for the analysis of reflection spectra [11, 12] allows one to estimate quantitatively the degree of skin reddening (erythema) and the percent content of basic chromophores in the skin such as oxyhemoglobin (HbO_2), deoxyhemoglobin (Hb), melanin, water, etc.

However, the above-mentioned methods cannot give a definite information on the size of the volume being measured. In this case, the determination of contributions introduced by different blood vessels to the detected reflection spectrum proves to be extremely complicated. As a result, the reflection spectra measured in experiments give information only on some mean values of bloodstream parameters (the degree of oxygenation, index of erythema, perfusion, etc.)

Our estimates of the spatial localisation of light multiply scattered in the skin and detected with a fibre sensor [13, 14] showed that the detection region contains a variety of blood vessels – from capillary loops to small veins and arteries. As the distance between the emitting and detecting optical fibres increases, the region of spatial localisation of a signal being detected expands to include not only skin tissues but also a part of muscles. Note that the use of optical fibre sensors is most preferable because they allow one to diaphragm the field of view of a photodetector to detect selectively the radiation scattered within the given observation angle at a certain point on the surface of a medium under study, thereby controlling the size of the volume being measured, which is important in the study of biological tissues.

In this paper, we simulate the reflection spectra of the human skin and compare them with the experimental

I V Meglinskii Department of Physics, N G Chernyshevskii Saratov State University, Astrakhanskaya ul. 83, 410026 Saratov, Russia; tel.: +7(845) 251 46 93; fax: +7(845) 224 04 46
Present address: School of Engineering, Cranfield University MK 43 0AL, UK; tel.: +44(1234) 75 47 67; fax: +44(1234) 75 04 25;
e-mail: i.meglinski@cranfield.ac. uk

Received 2 August 2001
Kvantovaya Elektronika **31** (12) 1101 – 1107 (2001)
Translated by M N Sapozhnikov

*Skin regions subjected to some change caused by some disease or some external thermal, chemical, or mechanical action.

reflection spectra detected with the help of a fibreoptic sensor. The attempts to simulate the reflection spectra of the human skin were made earlier in papers [15–17]. However, the diffusion approximation used in these papers substantially restricts the applicability of the results obtained. In addition, as mentioned above, to interpret the results quantitatively, one should know the region of spatial localisation of the detected signal and the contributions introduced by various parts of the vessel alveus and tissues in the region of localisation of probe radiation.

In our case, the diffusion approximation is invalid when the distance between the emitting and detecting optical fibres in a fibre sensor is small (250–800 μm) and is comparable with the geometric size of the radiation source and detector (100–200 μm). For this reason, we simulated the propagation of light in the multilayer, random, strongly scattering and absorbing medium and calculated the reflection spectra of the medium by the Monte Carlo method. The optical properties of skin tissues were simulated taking into account the spatially inhomogeneous distributions of blood, water, and melanin inherent in the human skin.

2. Simulation of light propagation in a random multilayer strongly scattering and absorbing medium

Taking into account the intricate inhomogeneous structure of the skin tissue [18, 19], we will simulate the human tissue by an inhomogeneous multilayer medium covering the half-space $z > 0$. The propagation of optical radiation in such a medium will be simulated by the Monte Carlo method, which combines the schemes for calculating real photon trajectories with the statistical weight method [13, 14]. To demonstrate some characteristic features of the Monte Carlo method, which distinguish this method from other models used for simulating the propagation of laser radiation in turbid strongly scattering random media [20–23], we consider some important aspects of the method.

The Monte Carlo simulation of propagation of optical radiation in a random multilayer strongly scattering and absorbing medium is usually based on a successive simulation of the trajectories of individual photon packets, beginning from their entrance to the medium until their departure from it. The conditions of inputting the photon packets into the medium and the conditions of their detection are determined by the diameters and numerical apertures of a source and a detector, as well as by their positions relative to the medium boundary. The trajectory of an individual photon packet in the medium is calculated by successively simulating the elementary events: reflection and refraction by the layer (medium) boundary, the mean free path, scattering, and absorption [20–23]. The probability of an elementary event is determined as a function of the optical parameters [8] of some or other layer of the medium: the absorption (μ_a) and scattering (μ_s) coefficients, the refractive index n, and the anisotropy factor g.

The mean free path l of a photon can take any positive values with the probability density [24]

$$p(l) = \mu_t \exp(-\mu_t l) = \mu_s \exp(-\mu_s l) \exp(-\mu_a l) + \mu_a \exp(-\mu_a l) \exp(-\mu_s l). \quad (1)$$

Here, $\mu_t = \mu_s + \mu_a$ is the extinction coefficient; the first term in the right-hand side of (1) describes the probability of photon scattering by a scattering centre, while the factor $\exp(-\mu_a l)$ characterises a decrease in this probability caused by possible absorption of the photon. The second term in (1) determines the probability of photon absorption in the medium and a possible change in this probability caused by scattering. We assume that radiation absorbed by the medium does not alter its optical properties, i.e., μ_a, μ_s, n and g. In this case, the photons absorbed by the medium are of no interest to us because the calculation of the reflection spectra involves only photons that reached the specified detection region after a random walk. In other words, the choice of the photon mean free path in the medium in the calculation of the reflection spectrum is determined only by the first term $\mu_s \exp(-\mu_s l) \exp(-\mu_a l)$ in equation (1).

This in turn allows the simulation of propagation of optical radiation in the scattering and absorbing medium in several steps. First, we calculate the trajectories of photon packets that arrived at the detection region in the non-absorbing medium ($\mu_a = 0$). All the trajectories detected are stored in the data file. The number of simulated trajectories depends on the specific conditions of the problem. In this paper, we detected 10^5 photon packets. Then, we take into account the absorption of the medium layers. For this purpose, following the trajectory of each individual photon packet, we recalculate its statistical weight coefficient (hereafter, the weight or the statistical weight) over the entire path of its random walk according to the absorption coefficient μ_a of the medium layers, i.e., by reducing the weight of the photon packet each time proportionally to $\exp(-\mu_a l)$:

$$W = W_0 \exp\left(-\sum_{k=1}^{N} \mu_a l_k\right), \quad (2)$$

where N is the number of free passages experienced by the photon packet between the scattering events; l_k is the photon mean free path between the $(k-1)$th and kth scattering events; W_0 and W are the initial and final statistical weights of the photon packet, respectively. It is obvious that the weight of the photon packet does not change in the absence of absorption in the medium.

Therefore, within the framework of this model, the radiation is scattered by scattering centres, whereas absorption occurs only between the successive scattering events, its probability being dependent on the photon path in the medium. Such a simulation of light propagation in random strongly scattering and absorbing media well agrees with the empirical Bouguer–Lambert–Beer law, which is used in analysis of spectrophotometric data:

$$D = -\ln\frac{I}{I_0} = \mu_a \sigma \rho + G, \quad (3)$$

where D is the optical density; ρ is the distance between a radiation source and a detector; σ is the differential factor of the photon path, which takes into account the elongation of the path of individual photons caused by multiple scattering of light in the medium; and G is a constant determined by the medium geometry and the position of the radiation source and detector with respect to the medium surface [25, 26].

In addition, the simulation of scattering and absorption in several steps allows one to take into account the wave properties of light at the interfaces of medium layers, including the attenuation of the incident radiation caused by reflection and refraction at Fresnel boundaries of the layers inside the medium. As shown in paper [14], despite strong multiple scattering at small distances between the radiation source and the detector, which are comparable with their size, the layer boundary and shape can substantially affect the spatial localisation of the detected signal and, hence, the shape of the reflection spectrum being simulated.

To obtain the best correspondence with the structure of a real object (in our case, the human skin), we represent the interface of the layers in the model medium in the form of wavy randomly periodic surfaces (Fig. 1), as has been proposed in paper [13]. In this case, the choice of the propagation direction of the photon packet and its change caused by refraction or reflection from randomly periodic layer interfaces are determined by the Fresnel formulas [27]. Thus, after reflection or refraction of the photon packet from the layer interface, its statistical weight reduces proportionally to the Fresnel reflection coefficient. As a result, the total weight of the photon packet arriving at the detection region is determined by the expression

$$W = \left[W_0 \prod_{j=1}^{M} R_j(\alpha)\right] \exp\left(-\sum_{k=1}^{N} \mu_a l_k\right), \tag{4}$$

where the function $R_j(\alpha)$ depends on the angle α upon the jth incidence of the photon packet at one of the layer interfaces and is determined by the Fresnel reflection (R) or transmission ($1 - R$) coefficient; M is the number of the events of interaction between the photon packet and layer interfaces.

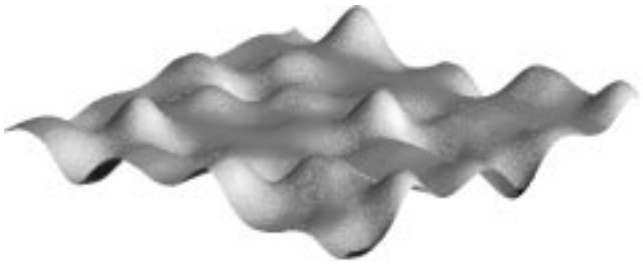

Figure 1. Example of a randomly periodical surface representing the interface between the epidermis layer and derma layers.

The attenuation of the radiation intensity caused by reflection from the medium boundary is taken into account by simulating the trajectories of photon packets reflected from the medium boundary one or more times. The trajectory of the photon packet is monitored until its statistical weight decreasing due to refraction and reflection at the layer and medium interfaces becomes smaller than the prescribed value 0.001.

The total radiation intensity I is determined as a sum of statistical weights of all photon packets arriving at the detector:

$$I = \sum_{q=1}^{N_{ph}} W_q.$$

The diffusion reflection coefficient R_d is defined as the ratio of the intensity I_0 of the incident radiation to the intensity I of the detected radiation:

$$R_d = \frac{I}{I_0} = \frac{1}{N_{ph}} \sum_{q=1}^{N_{ph}} \left(\prod_{j=1}^{M_q} R_j(\alpha)\right) \exp\left(-\sum_{k=1}^{N_q} \mu_a l_k\right). \tag{5}$$

Here, $I_0 = N_{ph} W_0$; N_{ph} is the total number of photon packets arriving at the detection region; N_q is the number of free passages performed by the qth photon packet between scattering events.

3. Choice of the optical parameters of human skin layers for calculating reflection spectra

Therefore, the simulation of scattering and absorption in several steps allows the rapid recalculation of the intensity of the detected signal for various sets of absorption coefficients of the medium layers from the calculated photon trajectories. In other words, the fragments of the reflection spectrum can be comparatively easily calculated within the specified wavelength range where the scattering properties of the medium (μ_s and g) remain unchanged. Because the scattering properties of the skin tissue change weakly in the visible range between 450 and 780 nm [28, 29], we can calculate the reflection spectrum of the skin in this spectral region.

For this purpose, we first determine the absorption spectrum of each layer, taking into account the absorbing elements contained in it:

$$\mu_a(\lambda) = \sum_{i=1}^{m} \left[\mu_a^{(i)}(\lambda) C_i \prod_{j=1}^{i-1} (1 - C_j)\right] + \mu_a^{(0)}(\lambda) \prod_{i=1}^{m} (1 - C_i), \tag{6}$$

where C_i is the volume concentration of the ith absorbing element in the given skin layer; m is the total number of absorbing elements contained in the layer; $\mu_a^{(i)}(\lambda)$ is the absorption coefficient of the ith absorbing element; $\mu_a^{(0)}$ is the background absorption coefficient caused by the intrinsic absorption of the medium in the absence of any absorbing elements.

We will consider oxyhemoglobin (HbO_2), deoxyhemoglobin (Hb), water, and melanin as absorbing elements (Fig. 2). It is known that absorption in the skin in the visible and near-IR spectral regions is determined by a combination of these absorbing elements. The absorption coefficients of Hb, HbO_2, and water presented in Fig. 2 were calculated from molar absorption spectra [30–33], whereas the absorption spectrum of melanin $\mu_a^{mel}(\lambda) = 5 \times 10^9 \lambda^{-3.33}$ was obtained by extrapolating the experimental data [34, 35]. Hereafter, the wavelength is expressed in nanometres. We assume that absorption caused by other components present in the skin tissue does not exceed the background absorption $\mu_a^{other}(\lambda)$, which, according to paper [36], can be described by the expression $\mu_a^{other}(\lambda) = 7.84 \cdot 10^7 \lambda^{-3.255}$ (Fig. 2).

Having found the main absorbing elements in the skin in this way, we calculate absorption coefficients for each of the

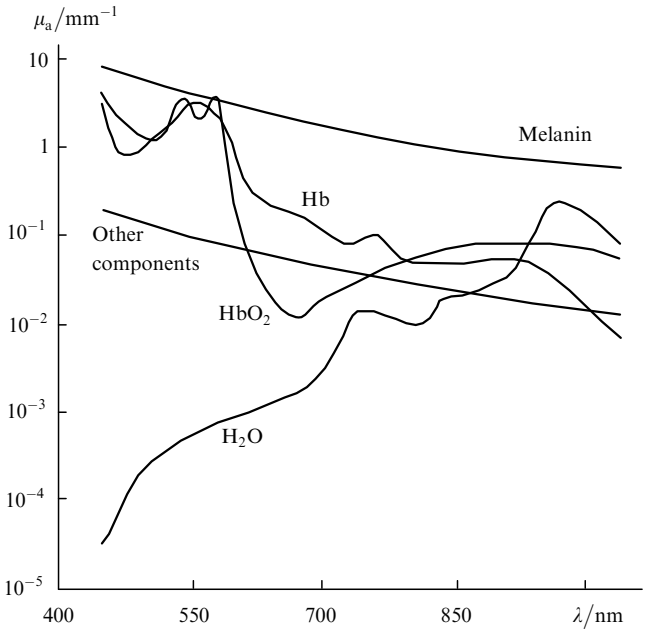

Figure 2. Absorption coefficients of main absorbing components of the human skin: oxyhemoglobin HbO_2, deoxyhemoglobin Hb, water, and melanin, and the absorption coefficient of other components of the skin.

layers using expression (6). The results of calculations are presented in Fig. 3. The volume concentration of absorbing elements in each of the layers is presented in Table 1. Note that the parameters presented in Table 1 were chosen according to the spatial distribution of main absorbing components of the skin, i.e., blood (blood vessels) [4, 37–40], water [41], and melanin [5, 18, 19]. The concentrations of Hb and HbO_2 in blood-containing skin layers were calculated from their volume content in the erythrocyte layer. Taking into account the degree of oxygenation S (see Table 1) determining the degree of domination of Hb over HbO_2 or of HbO_2 over Hb, equation (6) for blood-containing layers can be represented in the form

$$\mu_a(\lambda) = \gamma C_{blood}(1-S)\mu_a^{Hb} + \gamma C_{blood} S \mu_a^{HbO_2} + C_{H_2O}\mu_a^{H_2O} + (1-\gamma C_{blood})(1-C_{H_2O})\mu_a^{other}, \quad (7)$$

where μ_a^{Hb}, $\mu_a^{HbO_2}$ и $\mu_a^{H_2O}$ are the absorption coefficients of hemoglobin, deoxyhemoglobin, and water, respectively;

$$\gamma = F_{rbc} F_{Hb} H \quad (8)$$

is the parameter determining the total concentration of oxyhemoglobin and deoxyhemoglobin in the given blood volume; F_{rbc} is the volume concentration of erythrocytes in the total volume H of blood cells (hematocrit); and F_{Hb} is the total concentration of oxyhemoglobin and deoxyhemoglobin within one erythrocyte. The parameters S, F_{rbc}, and H can change from layer to layer [42–44], in particular, due to the influence of various physiological factors [43, 44]. Within the framework of this model, we use the values of parameters that are typical for the human blood [3, 4, 37–40, 42–44] (Table 1). The parameters $F_{rbc} = 0.99$ and $F_{Hb} = 0.25$ are the same for all the layers.

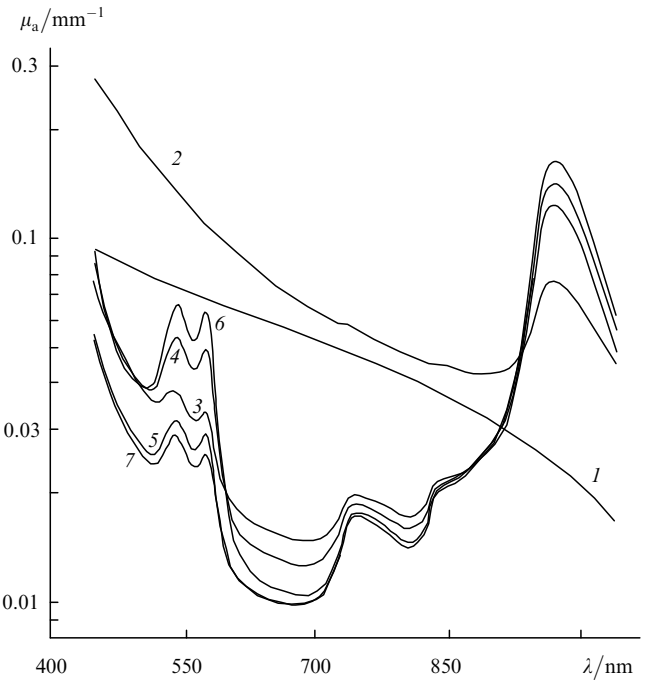

Figure 3. Absorption coefficients of model skin layers: *Stratum corneum* (*1*), epidermis (*2*), derma with capillary loops (*3*), derma with surface vessel interlacement (*4*), derma (*5*), derma with deep vessel interlacement (*6*), and hypodermic fat (*7*).

The absorption coefficient of the uppermost corneous skin layer (Stratum corneum) containing a great amount of keratin (Fig. 3) of thickness only 20 μm is described, according to (6), taking the experimental data [45] into account, by the expression

$$\mu_a^{sc}(\lambda) = [0.1 - 8.3\cdot10^{-4}\lambda + 0.125\mu_a^{other}(\lambda)] \times (1 - C_{H_2O}) + C_{H_2O}\,\mu_a^{H_2O}(\lambda). \quad (9)$$

The parameters characterising scattering and refraction in skin layers are presented in Table 2. These values of the parameters are typical for the normal human skin at a wavelength of 633 nm [13, 14].

Table 1. Contents of blood, water, and melanin in the human skin.

Layer	C_{mel}	C_{H_2O}	C_{blood}	S	H
Stratum corneum	0	0.05	0	–	–
Epidermis	0.1	0.2	0	–	–
Derma with capillary loops	0	0.5	0.04	0.6	0.4
Derma with surface vessel interlacement	0	0.6	0.08	0.6	0.45
Derma	0	0.7	0.05	0.6	0.45
Derma with deep vessel interlacement	0	0.7	0.14	0.6	0.5
Hypodermic fat	0	0.65	0.06	0.6	0.45

Table 2. Optical parameters of skin layers used in simulations.

Layer	μ_s/mm^{-1}	g	n
Stratum corneum	100	0.9	1.5
Epidermis	60	0.85	1.34
Derma with capillary loops	30	0.9	1.39
Derma with surface vessel interlacement	35	0.95	1.4
Derma	25	0.76	1.39
Derma with deep vessel interlacement	35	0.95	1.4
Hypodermic fat	15	0.8	1.44

4. Discussion of results

Fig. 4 presents the results of numerical simulation of the reflection spectra of the human skin obtained by the method described above. The simulation was performed for the case of a change in the blood content in upper (Fig. 4a) and deep (Fig. 4b) blood-containing skin layers by 40 % (see Table 1). The choice of the distances between the radiation source and the detector equal to 250, 400, and 800 μm was determined by the size of the fibre detector whose sensitivity region was analysed in papers [13, 14]. The diameters of the emitting and detecting optical fibres were 200 and 50 μm, respectively.

The results of the simulation well agree with the calculation of the localisation of the sensitivity region of the fibre sensor [13, 14] whose geometry was used in the simulation. As expected, the near-surface change in the blood content much stronger affects the reflection spectrum (Fig. 4a) than a change in the blood content in deep skin layers (Fig. 4b).

As the distance between the radiation source and the detector increases from 250 to 800 μm, the region of the detector sensitivity expands so that the influence of deep skin layers on the detected signal significantly increases. This results in a greater difference between the reflection spectra, which is manifested in the variation in the peak intensities in the regions between 500 and 600 nm and between 950 and 1050 nm (Fig. 4). A comparison of Figs 2 and 4 shows that the peaks observed in these spectral regions are related to blood and water, respectively. Note that the intensity of the peak caused by absorption in water observed in the 950–1050-nm region depends on the content of blood in upper skin layers (Fig. 4a).

The validity of the model used here and the adequate choice of the optical parameters of skin layers are illustrated in Fig. 5, where the model reflection spectrum and the reflection spectrum of the skin measured on the setup described in detail in papers [9, 46] are presented. The reflection was measured from the human skin on the rear side of the forearm. The distance between emitting and detecting fibres was 400 μm in both cases. The diameter of the core of fibres used in experiments was equal to that used in simulations.

Fig. 5 demonstrates good agreement between the model and experimental reflection spectra in the visible range between 450 and 650 nm. At the same time, these spectra noticeably differ from each other in the near-IR region between 650 and 1050 nm. This is explained by a decrease in

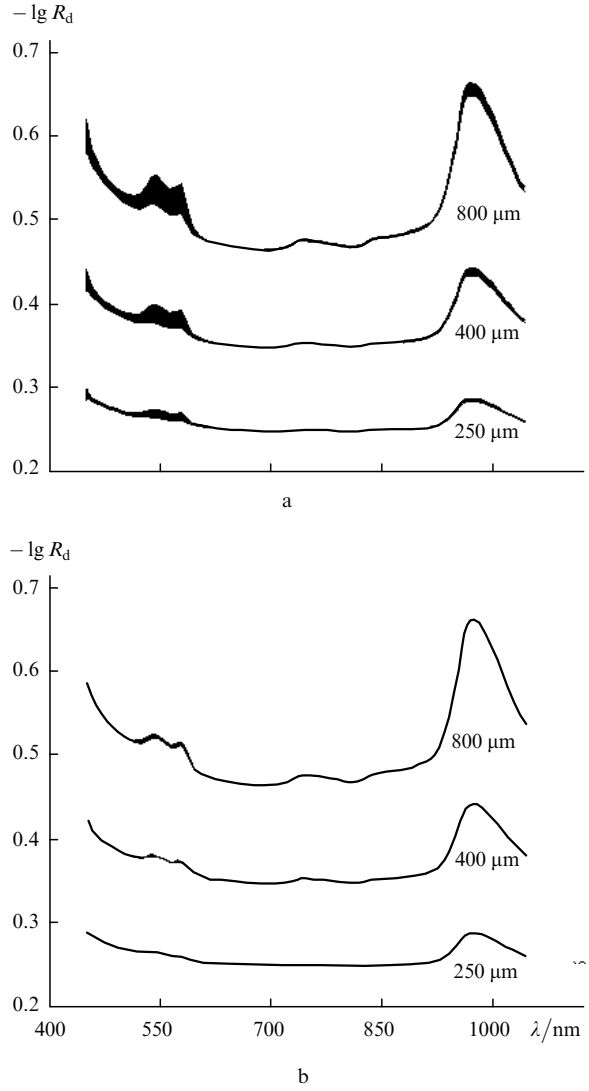

Figure 4. Reflection spectra of the human skin calculated by the Monte Carlo method for the blood content in the upper (a) and deep (b) skin layers changed by 40 % (see Table 1).

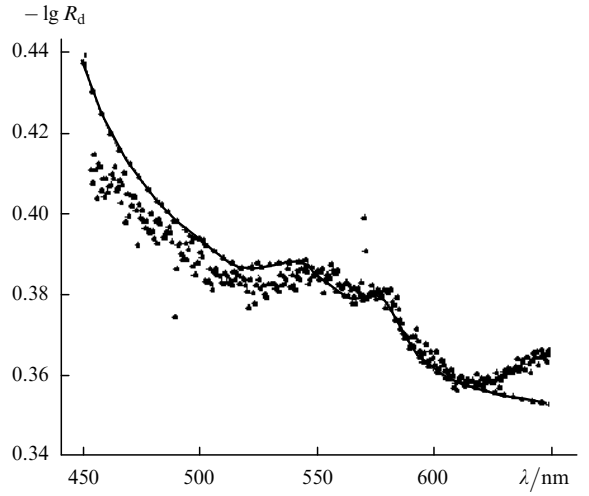

Figure 5. Experimental reflection spectrum of the human skin (dots) and its model reflection spectrum (curve).

the scattering coefficient of the skin in this spectral region. Recall that we assumed in our model that the scattering properties of skin layers are constant (see Table 2). Note that such a good agreement between the model and experimental spectra (Fig. 5) has been achieved to a great extent due to a proper choice of the main parameters determining the optical properties of model skin layers and their possible variations. Although this set of parameters is far from complete, nevertheless it is quite sufficient for the simulation of fragments of the reflection spectra of the human skin.

5. Conclusions

The reflection spectra of the human skin calculated in the paper are interesting from the point of view of the possibility of their decomposition into the absorption spectra of the main components of the skin. The results of simulations clearly demonstrate contributions of various parameters of the bloodstream in the given vessel alveus (layer) to the detected reflection spectrum. In addition, reflection spectra calculated for different input–output schemes for probe radiation can be used as calibration spectra for quantitative estimates of the degree of oxygenation of the skin blood and measurements of the content of various chromophores by the method of multilinear regression [11].

Note also that the prediction of changes in the optical properties of tissues caused by various biochemical, biophysical, and physiological processes is important for laser therapy and diagnostics in biology and medicine. The quantitative description of the dependence of the optical properties of the skin tissues on the parameters of the blood stream in the given vessel alveus is interesting from this point of view. This allows one to simulate and observe the dynamics of development of inflammatory and physiological processes, allergic reactions, and other variations occurring in skin tissues resulting in a change in the absorption coefficient (7). The method for simulating the propagation of optical radiation in multilayer strongly scattering and absorbing media can be also applied to the problems of materials technology, colloidal chemistry, etc.

Acknowledgements. This work was supported by the English Physical Studies and Research Council (EPSRC, Grant No. GR/L89433). The author thanks V V Tuchin and S J Matcher for useful advice and comments.

References

1. Priezzhev A V, Tuchin V V, Shubochkin L P *Lazernaya diagnostika v biologii i meditsine* (Laser Diagnostics in Biology and Medicine) (Moscow: Nauka, 1989)
2. Tuchin V V *Tissue Optics: Light Scattering Methods and Instruments for Medical Diagnosis* (Bellingham: SPIE Press, 2000), TT38
3. Ryan T J, in: *Physiology, Biochemistry, and Molecular Biology of the Skin*. (Ed. L A Goldsmith) (Oxford: Oxford University Press, 1991), vol. 2, p.1019
4. Kupriyanov V V, Karaganov Ya L, Kozlov V I *Mikrotsirkulyatornoe ruslo* (Microcirculation Alveus) (Moscow: Meditsina, 1975)
5. Chedekel M R, in: *Melanin: Its Role in Human Photoprotection* (Overland Park, Kansas: Valdenmar Publishing Co., 1995), p.11
6. Young A R *Phys. Med. Biol.* **42** 789 (1997)
7. Sinichkin Yu P, Utts S R, Meglinskii I V, Pilipenko E A *Opt. Spektrosk.* **80** 431 (1996)
8. Tuchin V V *Lazery i volokonnaya optika v biomeditsinskikh issledovaniyakh* (Lasers and Fibre Optics in Biomedical Studies) (Saratov: Izd. Saratov University, 1998), p. 384
9. Wallace V P, Crawford D C, Mortimer P S, Ott R J, Bamber J C *Phys. Med. Biol.* **45** 735 (2000)
10. Hajizadeh-Saffar M, Feather J W, Dawson J B *Phys. Med. Biol.* **44** 967 (1999)
11. Andersen P H, Bjerring P *Photodermatol. Photoimmunol. Photomed.* **7** 249 (1990)
12. Matcher S J, Elwell C E, Cooper C E, Cope M, Delpy D T *Anal. Biochem.* **227** 54 (1995)
13. Meglinskii I V, Matcher S D *Opt. Spektrosk.* **91** 330 (2001)
14. Meglinskii I V, Matcher S J *Med. Biol. Eng. Comput.* **39** 44 (2001)
15. Norvang L T, Fiskerstrand E J, Konig K, Bakken B, Grini D, Standahl O, Milner T E, Berns M W, Nelson J S, Svaasand L O *Proc. SPIE Int. Soc. Opt. Eng.* **2624** 155 (1995)
16. Kumar G, Schmitt J M *Proc. SPIE Int. Soc. Opt. Eng.* **2678** 442 (1996)
17. Kumar G, Schmitt J M *Appl. Opt.* **36** 2286 (1997)
18. Stenn K S, in: *Cell and Tissue Biology* (Ed. L Weiss) (Baltimore: Urban & Shwarzenberg, 1988), p.541
19. Odland G F, in: *Physiology, Biochemistry, and Molecular Biology of the Skin* (Ed L A Goldsmith) (Oxford: Oxford Univiversity Press, 1991), vol.1, pp. 3–62)
20. Keijzer M, Jaques S L, Prahl S A, Welch A J *Laser Surg. Med.* **9** 148 (1989)
21. Yaroslavskii I V, Tuchin V V *Opt. Spektrosk.* **72** 934 (1992)
22. Slovetskii S D *Radiotekhnika* **7** 73 (1994)
23. Wang L, Jacques S L, Zheng L *Comp. Methods Progr. Biomed.* **47** 131 (1995)
24. Sobol' I M *Metod Monte-Karlo* (Monte Carlo Method) (Moscow: Nauka, 1985), p. 80
25. Twersky V J. *Opt. Soc. Am.* **52** 145 (1962)
26. Twersky V J. *Opt. Soc. Am.* **60** 1084 (1970)
27. Born M, Wolf E *Principles of Optics*, 4th ed. (Oxford: Pergamon Press, 1969; Moscow: Nauka, 1973)
28. Doornbos R M P, Lang R, Aalders M C, Cross F M, Sterenborg H J C M *Phys. Med. Biol.* **44** 967 (1999)
29. Simpson C R, Kohl M, Essenpreis M, Cope M *Phys. Med. Biol.* **43** 2465 (1998)
30. Zijlstra W G, Buursma A, Meeuwsen van der Roest W P Clin. Chem. 37 1633 (1991)
31. van Assendelft O W *Spectrophotometry of Haemoglobin Derivatives* (Springfield: Thomas,1970), vol. 3, p. 355
32. Palmer K F, Willmans D *J. Opt. Soc. Am.* **64** 1107 (1974)
33. Hale G M, Querry M R *Appl. Opt.* **12** 555 (1973)
34. Anderson R R, Hu J, Parrish J A, in: Bioengineering and the Skin (Eds R Marks, P A Payne) (Lancaster: MTP, 1981), p. 253
35. Feather J W, Dawson J B, Barker D J, Cotterill J A, in: *Bioengineering and the Skin*, (Eds R Marks, P A Payne) (Lancaster: MTP,1981), p. 275
36. Saidi I S PhD (phys) thesis (Houston: Rice University, 1992)
37. Bull R, Ansell G, Stanton A W B, Levick J R, Mortimer P S *Int. J. Microcirc.* **15** 65 (1995)
38. Braverman I *J. Invest. Dermatol.* **93** S2 (1989)
39. Ikeda A, Umeda N, Tsuda K, Ohta S *J. Electron Microsc. Techn.* **19** 419 (1991)
40. Jaap A J, Shore A C, Stockman A J, Tooke J E *Diabetic Medicine* **13** 160 (1996)
41. Potts R *J. Soc. Cosmet. Chem.* **37** 9 (1986)
42. Levtov V A, Rigirer S A, Shadrina N Kh *Reologiya krovi* (Blood Reology) (Moscow: Meditsina, 1982)
43. Mchedlashvili G I *Mikrotsirkulyatsiya krovi: obshchie zakonomernosti regulirovaniya i narushenii* (Blood Microcirculation: General Properties of Control and Distortions) (Leningrad: Nauka, 1989)
44. Chizhevskii A L *Strukturnyi analiz dvizhushcheisya krovi* (Structural Aanalysis of Moving Blood) (Moscow: Izd. Akad. Nauk SSSR, 1969)

45. Sliney D, Wolbarsht M, in: *Safety with Lasers and Others Optical Sources. A comprehensive Handbook* (New York: Plenum Press, 1980), p.161
46. Mourant J R, Bigio I J, Jack D A, Johnson T M, Miller H D *Appl. Opt.* **36** 5655 (1997)